CARBON 46 (2008) 1892–1902

available at www.sciencedirect.com

ScienceDirect

journal homepage: www.elsevier.com/locate/carbon

Synthesis of different magnetic carbon nanostructures by the pyrolysis of ferrocene at different sublimation temperatures

*Qingfeng Liu, Zhi-Gang Chen, Bilu Liu, Wencai Ren, Feng Li Hongtao Cong, Hui-Ming Cheng**

Shenyang National Laboratory for Materials Science, Institute of Metal Research, Chinese Academy of Sciences, Shenyang 110016, PR China

ARTICLE INFO

Article history:
Received 30 April 2008
Accepted 29 July 2008
Available online 8 August 2008

ABSTRACT

Various magnetic nanostructures such as Fe nanoparticles (Fe-NPs) adhering to single-walled carbon nanotubes, carbon-encapsulated Fe-NPs, Fe-NP decorated multi-walled carbon nanotubes (MWCNTs), and Fe-filled MWCNTs have been synthesized by the pyrolysis of pure ferrocene. It is found that the formation of the nanostructures can be selectively controlled by simply adjusting the sublimation temperature of ferrocene, while keeping all other experimental parameters unchanged. Magnetic characterization reveals that these nanostructures have an enhanced coercivity, higher than that of bulk Fe at room temperature. Based on the experimental results, the formation mechanism of the nanostructures is discussed in detail.

1. Introduction

Recently, magnetically-functionalized carbon nanostructures have attracted an increasing interest, due to their unique electronic, magnetic and nonlinear optical properties, as well as many potential applications in biomedicines, magnetic data storage devices, magnetic force microscopy, and nanoscale electronics [1–5]. The generation of small and bare magnetic metals such as nanoparticles (NPs) and nanowires has been proved to be difficult due to the easy oxidation tendency of metals such as Fe, Co and Ni [6]. The idea of encapsulating them within carbon shells, which ensure that magnetic metals are retained in a reduced state, seems feasible. In addition, beyond the geometrical advantage of sphere/cylinder-shaped nanostructure design, carbon shells provide an effective protection against environmental oxidation and thus maintain long-term stability of the ferromagnetic core [7,8]. For such purpose, many methods including detonation-induced reaction [9], arc discharge [10], and chemical vapor deposition (CVD) [11] have been developed for synthesis of various magnetic carbon nanostructures. In most growth processes, metallocenes such as ferrocene are frequently used as precursors to prepare magnetic carbon nanostructures, because they can not only act as carbon source, but also give rise to small metal clusters as catalyst and the magnetic properties of the final products [12,13]. However, the formation of various nanostructures such as NPs, nanowires, heterostructures, and carbon nanotubes (CNTs) by the pyrolysis of ferrocene has painted a considerably complex picture about their selectivity and growth mechanism, which are not yet completely understood [12–16].

In this paper, we have developed a simple and effective method for synthesis of Fe nanoparticles (Fe-NPs) adhering to single-walled carbon nanotubes (SWCNTs), carbon-encapsulated Fe nanoparticles (CNPs), Fe-NP decorated multi-walled carbon nanotubes (MWCNTs), and Fe-filled MWCNTs by the pyrolysis of pure ferrocene by only controlling its sublimation temperature (T_{sub}). The magnetic characterization shows that these samples have an enhanced coercivity at room temperature. Understanding of the important role of T_{sub} can give valuable information for an insight into the growth mechanism of these nanostructures, which will help

* *Corresponding author:* Fax: +86 24 2390 3126.
E-mail address: cheng@imr.ac.cn (H.-M. Cheng).
0008-6223/$ - see front matter
doi:10.1016/j.carbon.2008.07.038

us to improve the selectivity and CVD growth efficiency of various carbon nanostructures.

2. Experimental

The synthesis was performed in a quartz tube reactor (i.d. 40 mm) inside a dual-zone furnace. In our experiments, the T_{sub} of the ferrocene was finely controlled, varying from 60–400 °C within a 5-°C-temperature range while keeping all other experimental parameters such as growth temperature and flow rate of carrier gas unchanged. When the temperature in the second zone reached ~1100 °C, a known quantity of pure ferrocene was sublimated at the scheduled T_{sub} in the first zone. Ferrocene vapor was carried into the second zone, where pyrolysis occurred, by ~2000 sccm Ar flow (carrier gas). After the growth, the furnace was cooled naturally to room temperature under the protection of Ar.

The samples were characterized by using scanning electron microscope (SEM, LEO SUPRA35), X-ray diffractometer (XRD, CuK_α), transmission electron microscope (TEM, JEOL2010 and TecnaiG2 F30), micro-Raman microscope (Jobin Yvon LabRam HR800), thermogravimetric analyzer (TGA, NETZSCH STA 449C) and superconducting quantum interference device (SQUID) magnetometer.

3. Results and discussion

3.1. Morphological and structural features of magnetic carbon nanostructures by the pyrolysis of ferrocene by controlling T_{sub}

SEM and TEM were used to examine the morphology and structure of the samples produced by the pyrolysis of ferrocene. At a low T_{sub} of 90 °C, the pyrolysis of ferrocene yields semi-transparent and web-like carbon deposit, which attaches to the quartz tube reactor at the outlet end. The deposit comprises abundant Fe-NPs adhering to CNTs with tens of micrometers in length (Fig. 1a). EDX analysis reveals that that the sample has a C/Fe atomic ratio of 2–3. In order to obtain the morphology of the sample, a piece of the transparent film formed during synthesis was attached onto a copper grid and then fixed by several drops of ethanol for TEM observation, as shown in Fig. 1b. A prominent feature is that a great number of Fe-NPs are adhered to SWCNT bundles. Fig. 1c shows a typical TEM image of the sample after sonication in ethanol for 2 h, demonstrating the tight adherence of Fe-NPs to SWCNTs. Meanwhile, the small intensity ratio of D to G band (I_D/I_G) reveals that the high quality of the SWCNTs (Fig. 1d). However, Fig. 1e indicates that the SWCNTs are very easily oxidized in

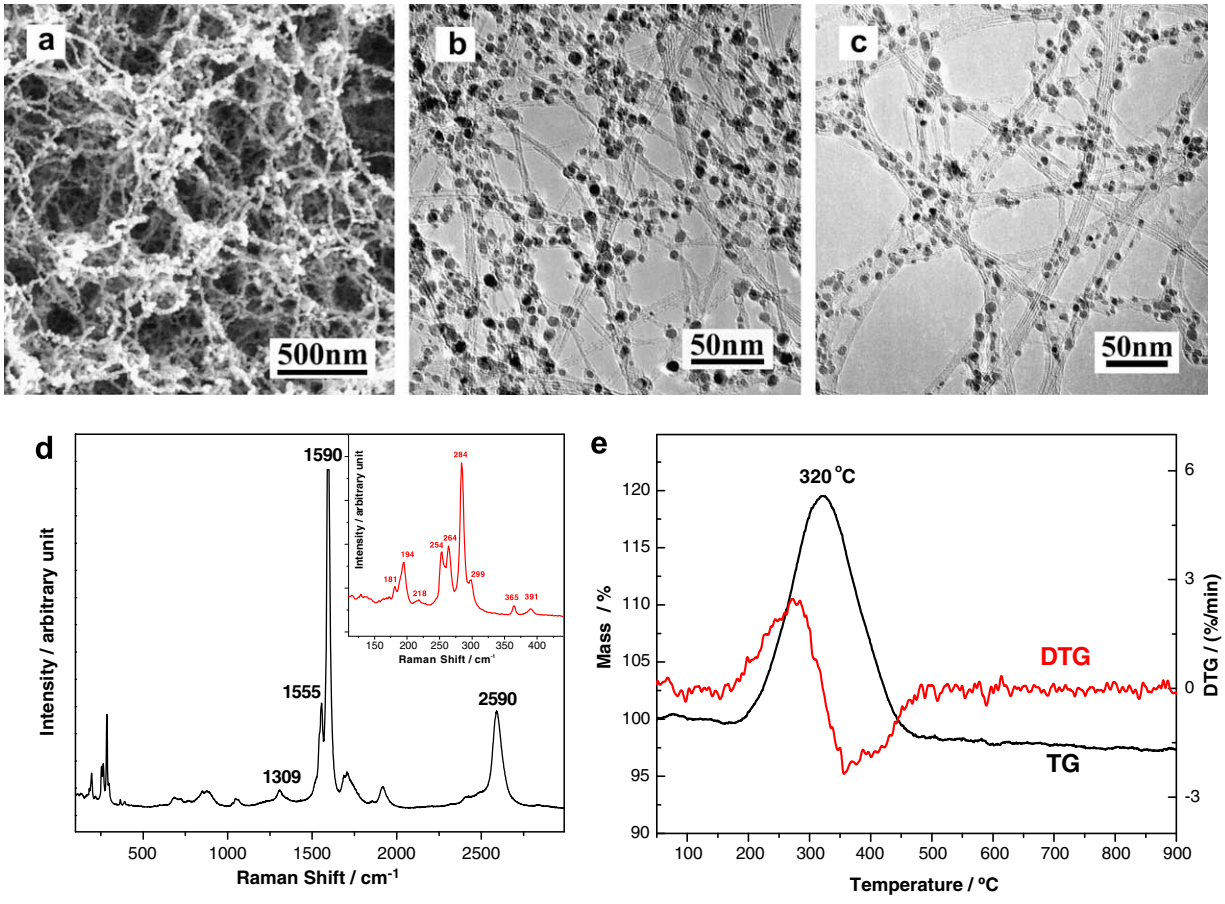

Fig. 1 – (a) SEM image of Fe-NPs adhering to SWCNTs produced by the pyrolysis of ferrocene at T_{sub} of 90 °C. (b–c) TEM images of the Fe-NPs adhering to SWCNTs (b) before and (c) after sonication treatment for 2 h. (d) Raman spectra of the Fe-NPs adhering to SWCNTs excited by a laser of E_{laser} = 1.96 eV. Inset in (d) is the corresponding radial breathing mode (RBM). (e) TGA curves of the Fe-NPs adhering to SWCNTs with a heating rate of 10 °C/min in the airflow.

an airflow in the presence of abundant Fe-NPs, because transition metals is known to catalyze the gasification of carbon, although the mechanism is not fully understood [17]. The residual metal oxide (i.e. mainly Fe_2O_3) is about 97 wt%, which is in agreement with EDX analysis.

At T_{sub} of ~130 °C, the pyrolysis of ferrocene tends to produce black powder, consisting of uniform spherical NPs, as shown in Fig. 2a. Fig. 2b reveals that the great majority of this sample is CNPs, with a core-shell structure of an iron core and carbon shells. The carbon shells tightly surround the iron core without any obvious voids (the inset in Fig. 2b), ensuring long-term stability of the iron core. To validate such protection of graphitic shells on the encapsulated iron core, the as-synthesized CNPs were immersed in concentrated HNO_3 (~65 wt%) for 30 h at room temperature. Fig. 2c shows a typical TEM image of the resulting CNPs in a large quantity. The Fe-C core-shell structures remained after the HNO_3 treatment (Fig. 2d). The iron core is crystalline and has a lattice fringe spacing of 0.20 nm, related to the (110) plane of the α-Fe crystal (JCPDS06-0696); the spacing of the lattice fringes of shells is 0.34 nm, which is close to that of the graphite (002) plane.

When ferrocene is sublimated at ~150 °C, Fe-NP decorated CNTs are obtained in a large quantity, as shown in Fig. 3a. Fig. 3b shows that the sample consists of MWCNTs homogeneously and densely decorated by numerous Fe-NPs on their outer surface. The MWCNTs are decorated by Fe-NPs with several micrometers (~ 5.5 μm) in length, as shown in Fig. 3c. The internal cavities of these MWCNTs are either empty or intermittently filled by short Fe nanowires. It is worth noting that preparation of this specimen for TEM observation involved sonication in ethanol. However, even after long-time sonication for hours, the Fe-NPs are not peeled off from the outer surface of MWCNTs, indicating that the Fe-NPs are tightly anchored onto the outer surface of MWCNTs. Obviously, the strong interaction between the Fe-NPs and the surface of MWCNTs will be advantageous when such a nanostructure is used as support for heterogeneous nanocatalysts in liquid-phase reactions for magnetic separation [18].

At T_{sub} of 280 °C, many flake-like films are produced. These films are aligned Fe-filled MWCNTs with ~10 μm in length (Fig. 4a). The MWCNTs can be continuously filled by very long Fe nanowires of ~5 μm in length (Fig. 4b), much longer than the previously-synthesized Fe-filled MWCNTs [6–8, 12–14]. Moreover, the diameters of the MWCNTs and Fe nanowires are found to increase with the increase of T_{sub} from 160 to 400 °C, as shown in Fig. 5.

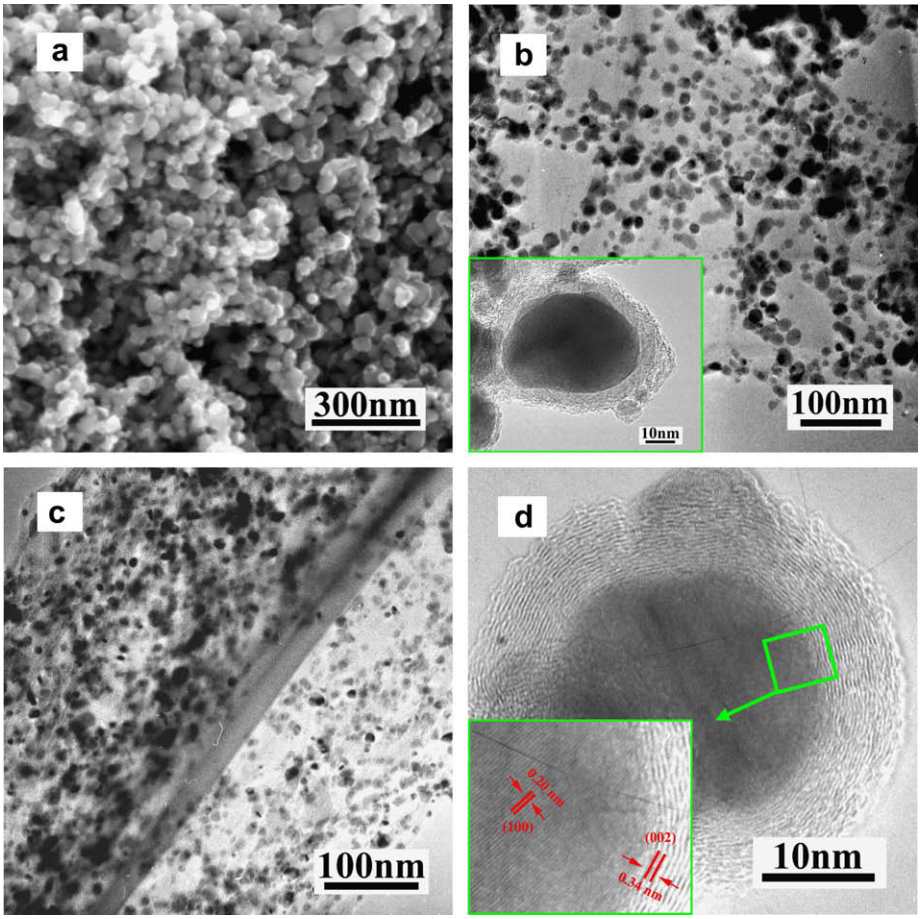

Fig. 2 – (a) SEM and (b) TEM images of the CNPs produced by the pyrolysis of ferrocene at T_{sub} of 130 °C. Insert in (b) is an enlarged TEM image of a CNP. (c–d) TEM images of the resulting CNPs after the HNO_3 treatment for 30 h at room temperature. Insert in (d) is an enlarged TEM image of the framed portion of (d).

Based on our experiments in general, Fe-NPs adhering to SWCNTs, CNPs, Fe-NP decorated MWCNTs, and Fe-filled MWCNTs were produced by the pyrolysis of ferrocene by controlling its T_{sub} in the temperature ranges of 60–110, 110–140, 140–160 and 160–400 °C, respectively, while keeping all other experimental parameters unchanged. It should be noted that although these as-synthesized nanostructures correspond very well to the above T_{sub} ranges, the pyrolysis of ferrocene simultaneously yielded very small quantities of other structures in such T_{sub} ranges. Moreover, at the boundary temperature of these T_{sub} ranges, both corresponding structures are mainly formed by the pyrolysis of ferrocene. For example, when ferrocene is sublimated at 110 °C, the SWCNTs are still produced; however, CNPs are also formed in a large quantity

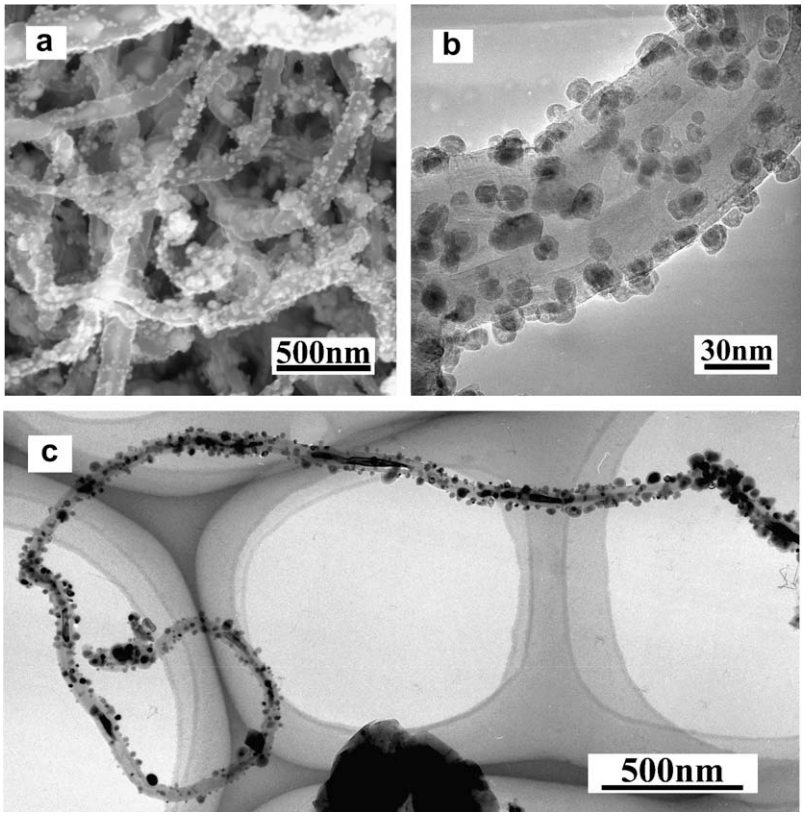

Fig. 3 – (a) SEM and (b–c) TEM images of Fe-NP decorated MWCNTs produced by the pyrolysis of ferrocene at T_{sub} of 150 °C.

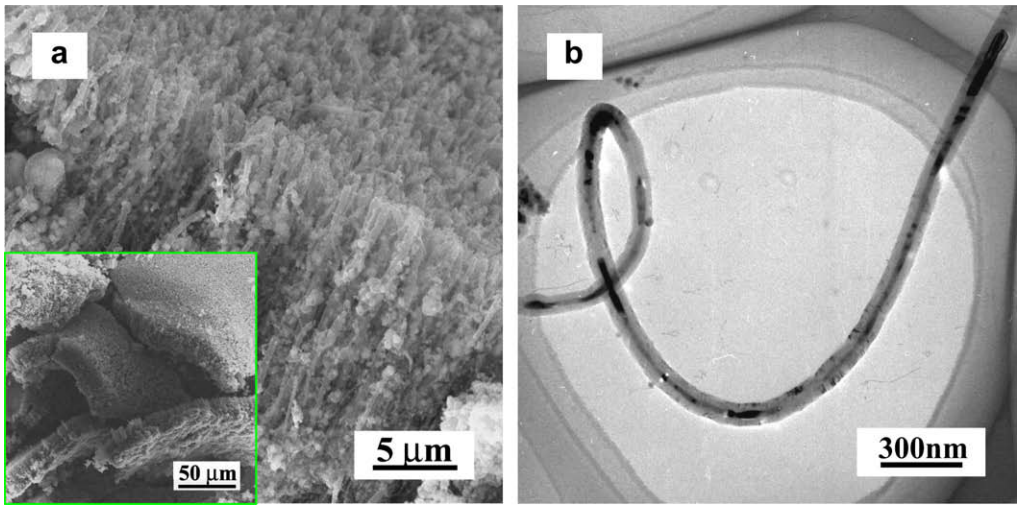

Fig. 4 – (a) SEM and (b) TEM images of Fe-filled MWCNTs produced by the pyrolysis of ferrocene at T_{sub} of 280 °C. Insert in (a) is a low-magnification SEM image.

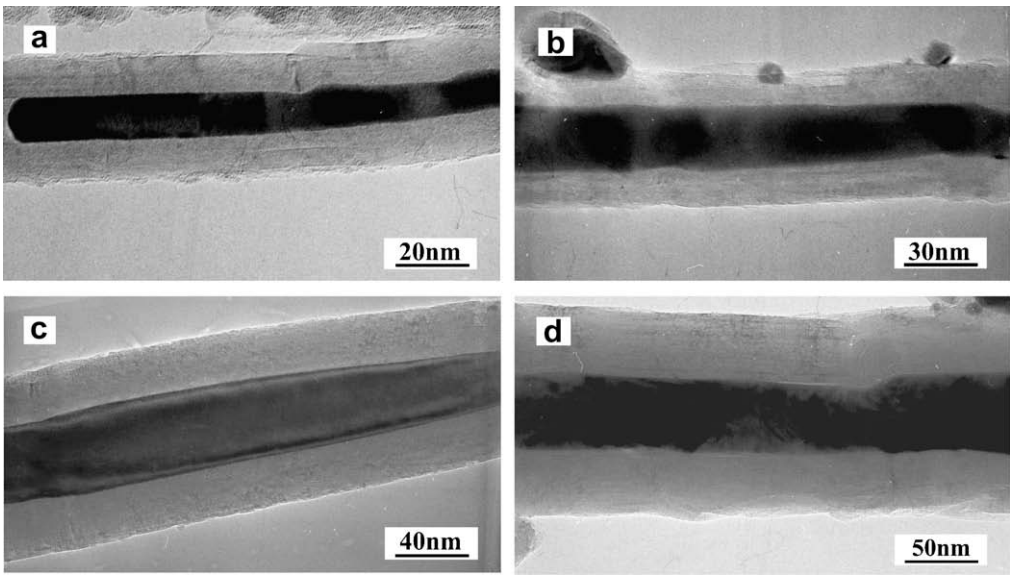

Fig. 5 – (a–d) TEM images of typical Fe-filled MWCNTs by the pyrolysis of ferrocene at T_{sub} of (a) 170, (b) 240, (c) 320 and (d) 380 °C.

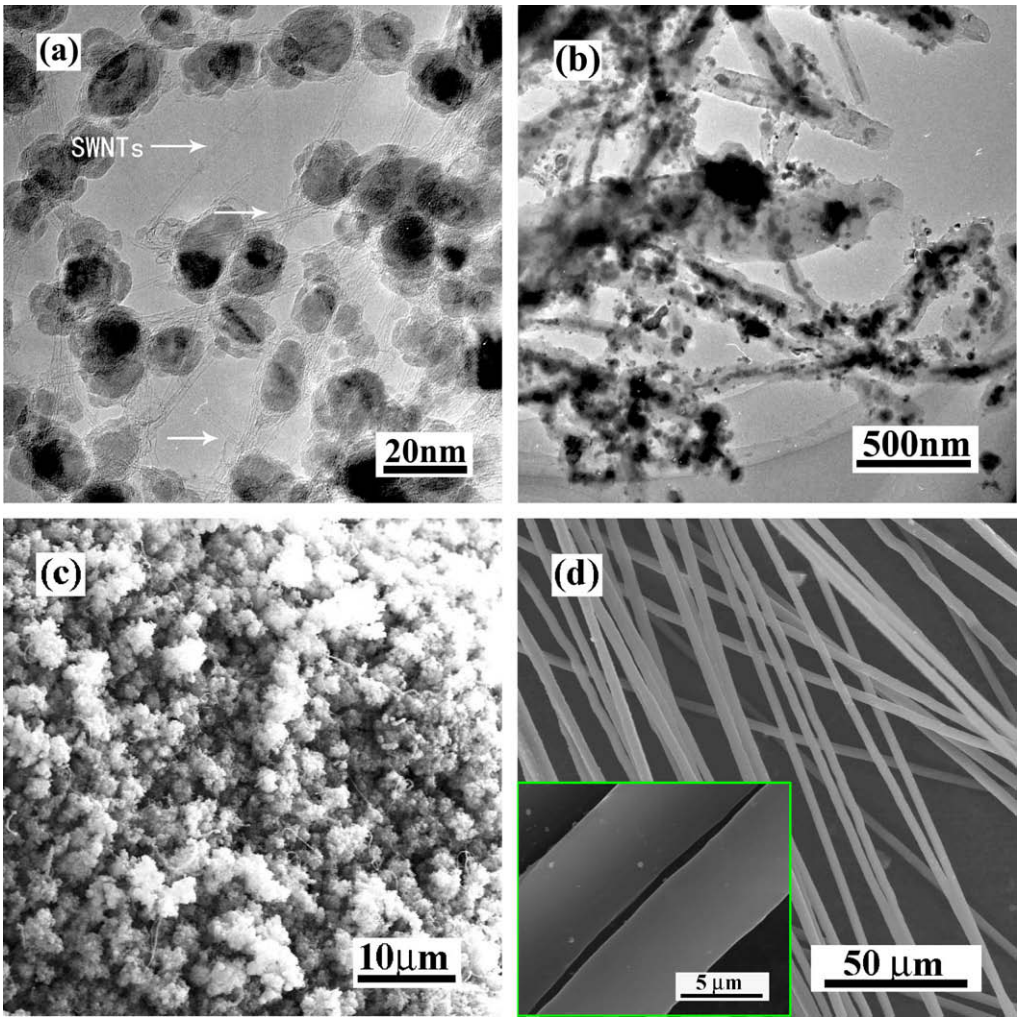

Fig. 6 – (a–b) TEM and (c) SEM images of typical products by the pyrolysis of ferrocene at T_{sub} of (a) 110, (b) 160 and (c) 450 °C. (d) SEM image of carbon fibers accumulated at the center of the quartz reaction tube by the pyrolysis of ferrocene at T_{sub} ranging from 200 to 400 °C due to the flow fluctuations of carrier gas. Insert in (d) is an enlarged SEM image of two carbon fibers.

by the pyrolysis of ferrocene, as shown in Fig. 6a. At T_{sub} of 160 °C, the pyrolysis of ferrocene tends to produce more Fe-filled MWCNTs instead of Fe-NP decorated MWCNTs (Fig. 6b). On the other hand, once T_{sub} is over 450 °C, only bulk C/Fe mixtures (Fig. 6c) are formed in a large quantity, with a few small spherical or tubular structures. Meanwhile, under certain conditions, the flow fluctuations of carrier gas can result in many long and straight carbon fibers (Fig. 6d) to be produced and accumulated at the center of the quartz reaction tube from the pyrolysis of ferrocene at T_{sub} ranging from 200 °C to 400 °C.

3.2. *Characterization of iron in carbon nanostructures and their corresponding magnetic properties*

The formation mechanism of magnetic carbon nanostructures by the pyrolysis of ferrocene is not yet completely understood, although a vapor-liquid–solid mechanism may be involved with filling of metals in a liquid state [19]. The particular shape, size and structure of products appear to be strongly determined by the quantity and dimensions of metal particles remaining after the pyrolysis of ferrocene. As a result, in order to explore the growth mechanism of magnetic carbon nanostructures by the pyrolysis of ferrocene, it is necessary to examine the metal particles in these products.

Fig. 7a shows the XRD diffraction patterns of these samples. The peak at about 26.2° can be assigned to the (002) plane of hexagonal graphitic structure with an interlayer spacing of 0.34 nm. This peak is symmetric and narrow, indicating a high crystallinity of these samples. The peaks at 44.7°, 65.0° and 82.3° can be identified as the (110), (200) and (211) planes of body-centered cubic (bcc) lattice, i.e. α-phase, respectively. The peak intensities and positions quantitatively confirm that α-Fe phase, thermodynamically favorable at room temperature and ambient pressure, dominates in all samples, though a fraction of orthorhombic cementite Fe_3C phase is also seen in the XRD diffraction patterns. The face-centered cubic (fcc) γ-Fe (< 5%) in Fe-filled MWCNTs cannot be ruled out, although not seen in the XRD diffraction patterns [19]. In spite of thermodynamic instability of γ-Fe phase at low temperatures, it may be retained in iron nanowires encapsulated in CNTs due to the confinement effects (~1 TPa) of the surrounding carbon shells [20].

Fig. 7b shows the Fe-NP diameter distribution in the range of 2-13 nm and the Gaussian mean diameter of 7.2 nm for Fe-NPs adhering to SWCNTs. Direct observation on the Fe-NPs as catalyst for the nucleation of SWCNTs reveals that they have also a similar diameter distribution of 2–13 nm. Fig. 7c shows the diameter distribution in the range of 12–44 nm and a Gaussian mean diameter of 22 nm for CNPs. With the increase of T_{sub} (~150 °C), the size of metal particles as catalyst for the nucleation of MWCNTs further becomes larger. Interestingly, the average size of Fe-NPs that do not act as catalyst but decorate on the surface of MWCNTs is ~10 nm (Fig. 7d). When T_{sub} is over 160 °C, more ferrocene molecules are carried into the reaction zone, and their subsequent pyrolysis

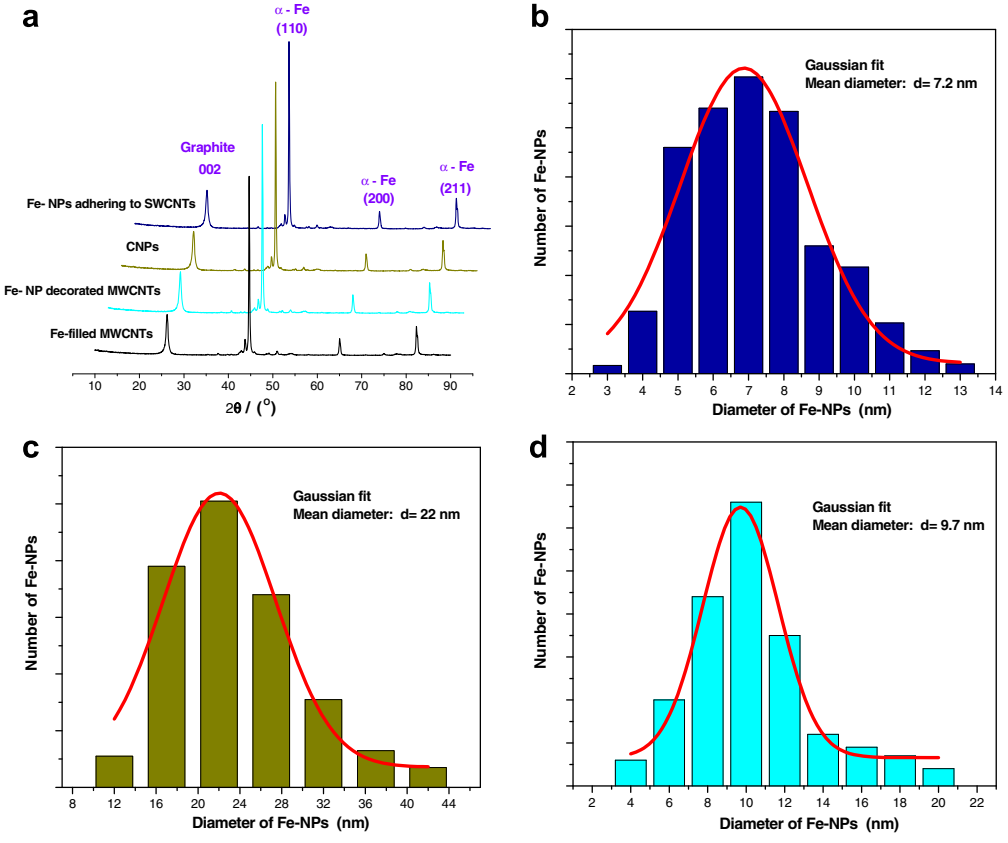

Fig. 7 – (a) XRD patterns of carbon nanostructures. (b–d) Fe-NP diameter distributions for (b) Fe-NPs adhering to SWCNTs, (c) CNPs, and (d) Fe-NP decorated MWCNTs.

produces abundant Fe clusters, which agglomerate into nanowires within nanotube channels. Therefore, it can be concluded that the higher the T_{sub} is, the larger the size of catalysts or even long metal nanowires are produced by the pyrolysis of ferrocene.

To understand the magnetic properties of the samples, SQUID magnetometer was used for magnetic characterization of these carbon nanostructures at room temperature. Fig. 8a shows an enhanced coercivity (H_c) of 163 Oe for Fe-NPs adhering to SWCNTs, higher than that ($H_c = \sim 1$ Oe) of bulk iron, which is ascribed to the large surface anisotropy effect [21] and the strong interactions between magnetic NPs that can lead to ordering of magnetic moments [22]. It is worth noting that the H_c of this sample is nearly four times of the value (H_c=45 Oe) of arc-synthesized similar structure [23]. The possible reason is that arc-induced superhigh plasma temperature more favors the formation of Fe_3C and γ-Fe phases than the moderate CVD growth temperatures [17]. Fig. 8b shows a smaller H_c of 135 Oe for the CNPs, due to the random arrangement and larger size of the CNPs. The H_c of 397 Oe for Fe-NP decorated MWCNTs (Fig. 8c) and H_c of 472 Oe for Fe-filled MWCNTs (Fig. 8d) are far larger than that of CNPs. A reasonable explanation is that Fe decorated on the outer surface of MWCNTs or filled in the inner channel of MWCNTs is arranged in a quasi-one-dimensional manner [23]. On the other hand, the saturation magnetization (M_s) of each sample is much lower than that (M_s = 222 emu/g) of bulk iron, because of the small dimensions of Fe in these samples.

3.3. Formation mechanism of different carbon nanostructures by the pyrolysis of ferrocene by controlling T_{sub}

T_{sub} of ferrocene in the first zone plays a decisive role in the formation of different carbon nanostructures, because all other experimental parameters are unchanged. In our experiments, carbon is relatively insufficient while Fe is superfluous, because both of them are derived from the only source, i.e. ferrocene. In the reaction process, only a very small portion of iron acts as catalyst for absorption or dissociation of gas-phase reactants, while most of the remaining iron is attached to, decorated on, or filled in the formed nanostructures. Moreover, the higher the T_{sub} is, the larger the size of catalyst is produced by the pyrolysis of ferrocene. Meanwhile, the size of catalyst is closely related to the structure of final product; e.g. small particles yield SWCNTs, while large ones are covered by graphitic layers or give rise to MWCNTs. Based on the experimental results, the formation of various carbon nanostructures by the pyrolysis of ferrocene by controlling T_{sub} is schematically depicted in Fig. 9.

Fig. 10 shows that the sublimation rate of ferrocene strongly depends on the temperature and the heating rate. Different T_{sub} of ferrocene can lead to different sublimation rates, and then vaporizes different quantities of ferrocene molecules into the second zone, in which ferrocene quickly decomposes and yields different ambient particulate concentrations with the fixed molar ratio of C/Fe = 10/1. When ferrocene is sublimated slowly at low temperatures (<110 °C), only

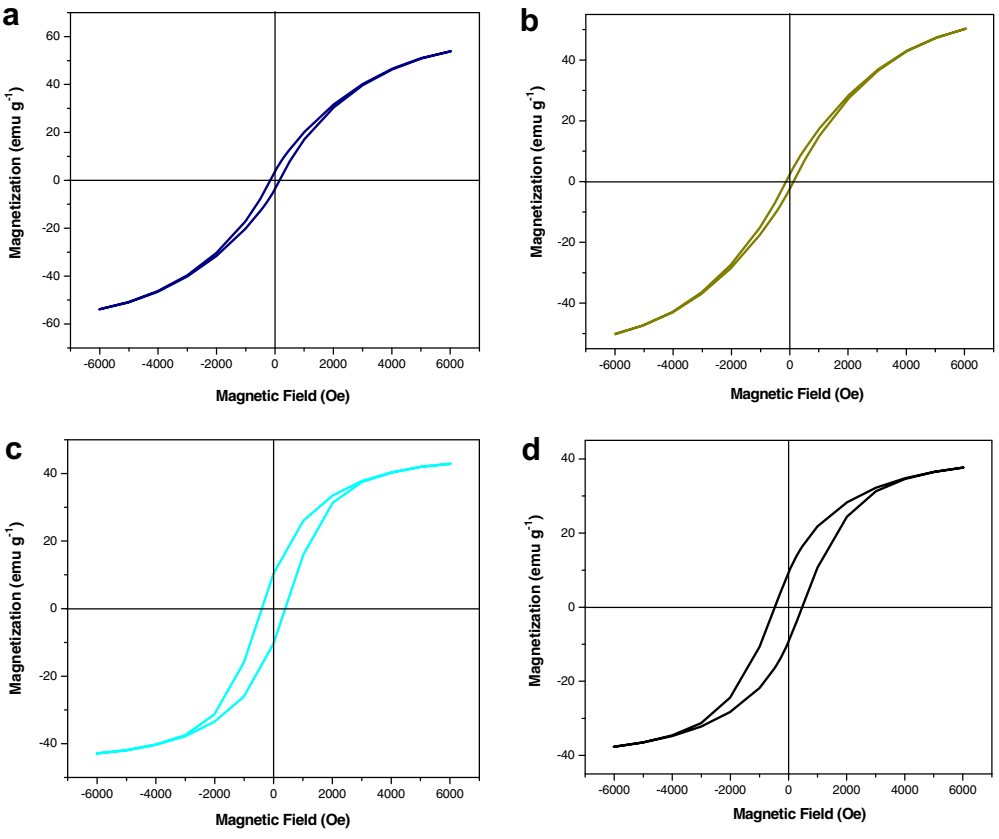

Fig. 8 – (a–d) Hysteresis loops measured at room temperature for (a) Fe-NPs adhering to SWCNTs, (b) CNPs, (c) Fe-NP decorated MWCNTs, and (d) Fe-filled MWCNTs.

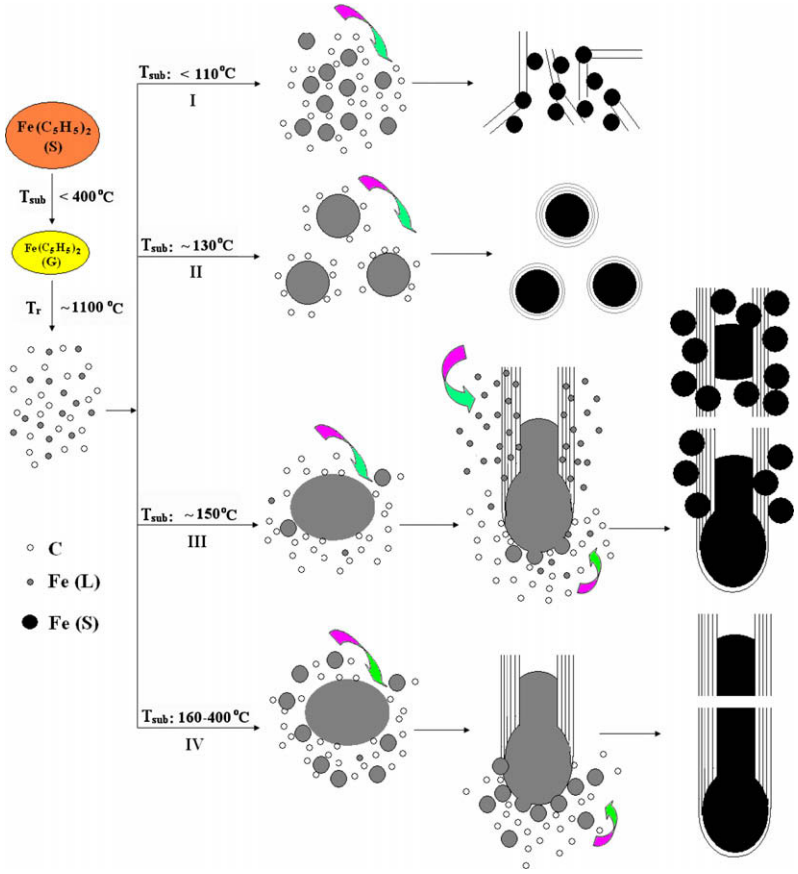

Fig. 9 – Schematic of the formation mechanism of magnetic carbon nanostructures by the pyrolysis of ferrocene by controlling T_{sub}.

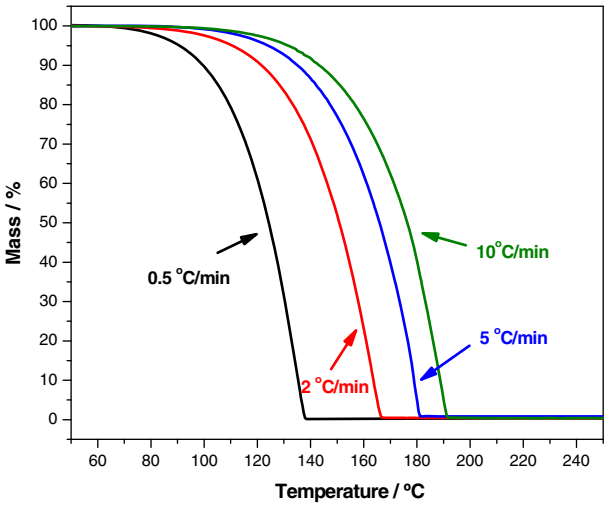

Fig. 10 – TGA curves of ferrocene with various heating rates in the Ar flow.

a small quantity of ferrocene is carried into the reaction zone by the gas flow, and its subsequent pyrolysis produces tiny Fe-NPs (<10 nm), some of which act as catalyst for the nucleation and growth of SWCNTs, while the rest are tightly attached to SWCNTs. When T_{sub} is in the range of 110–130 °C, the formed Fe-NPs (~20 nm) are beyond the size limit suitable for the growth of SWCNTs, but fall into the size range suitable for the nucleation of MWCNTs. However, under such condition, the carbon concentration is deficient for the growth of MWCNTs, and then CNPs are mainly produced. Therefore, a logical question is why SWCNTs instead of smaller CNPs are still formed from more deficient carbon by the pyrolysis of ferrocene at T_{sub} of ~90 °C. We believe that a lower carbon supply will allow the structures to form more slowly, giving each carbon atom more time to anneal to its lowest energetic configuration. In a comparable diameter range, the activation energy of CNPs is higher than that of SWCNTs but lower than that of MWCNTs. Therefore, SWCNTs instead of CNPs were formed when ferrocene was sublimated at <110 °C. Our results are well in agreement with the theoretic calculation by Hafner et al [24].

As the carbon concentration increases with T_{sub}, MWCNTs begin to be formed and grown from Fe catalyst particles. Meanwhile, more Fe-NPs are produced to deposit on the sidewalls of the newly-produced MWCNTs due to the strong affinity between C and Fe. The decorated Fe-NPs on the surface of MWCNTs have an average diameter of ~10 nm, smaller than that of the CNPs. Once T_{sub} is over 160 °C, great quantities of carbon are supplied to the second zone, and so abundant MWCNTs are produced. As the reaction proceeds, more and more iron clusters are also simultaneously supplied to the second zone and aggregate into long nanowires to be filled in the internal cavities of MWCNTs.

To reveal how iron enters the inner cavities of nanotubes, we examined Fe-filled MWCNTs obtained after different reaction duration times. Fig. 11 shows the growth evolution of Fe-filled MWCNTs with different lengths. It can be seen that MWCNTs lengthen with a close tip, concurrent with the filling of iron in internal cavities of nanotubes. It is suggested that the growth of Fe-filled MWCNTs predominantly follows the base growth mode, where carbon is successively supplied to the catalyst particle to form a nanotube, and simultaneously, iron clusters incessantly aggregate into the catalyst particle to supply the material to be filled in the internal cavities of the growing nanotube, as schematically shown in the IV section of Fig. 9. However, a key question is what the driving force is to draw iron into the inner cavities of MWCNTs, which involves the surface energies of the interaction between the liquid Fe and the solid surface of the nanotube such as the capillarity.

As known, if one wants to fill a nanotube with a given material by capillarity, the material must have a contact angle <90°, since this is a problem of wetting that is intimately related with capillarity. However, since the contact angle of liquid iron on nanotube walls is >90°, liquid iron cannot wet and enter MWCNTs by capillarity without the aid of an external force. Wei et al. believed that the aid of flow fluctuations made iron to overcome the surface tension and then be encapsulated in MWCNTs [25]. If pure Fe is to be introduced into MWCNTs, the pressure required will depend on the diameter of the tube and the contact angle, as can be understood from the Laplace equation:

$$\Delta P = 2\gamma \cos\theta / r \tag{1}$$

Where ΔP is the pressure difference across the liquid-vapor interface, r is the radius of curvature, γ is the surface tension, and θ is the liquid–solid contact angle. Based on TEM observations, the contact angle of liquid iron on MWCNT walls is ~135 °C. And the surface tension of the liquid iron, γ measured in Nm^{-1}, can be calculated as follows [26]:

$$\gamma = 2.858 - 0.00051T \tag{2}$$

where T is the temperature in Kelvin. Thus, at 1100 °C where Fe-filled MWCNTs grow, $\gamma = 2.158\ Nm^{-1}$. According to Eq. (1), to fill a 50-nm-diameter nanotube with liquid Fe, outside pressure of an order of ~610 atm will be required, depending on the contact angle. If the sample is cooled with this pressure on, the Fe will be stuck inside the nanotubes. Although the surface tension will be lower at higher temperatures of the arc, the filling pure iron is still not most likely a result of capillary action. So it is hard to imagine that just flow fluctua-

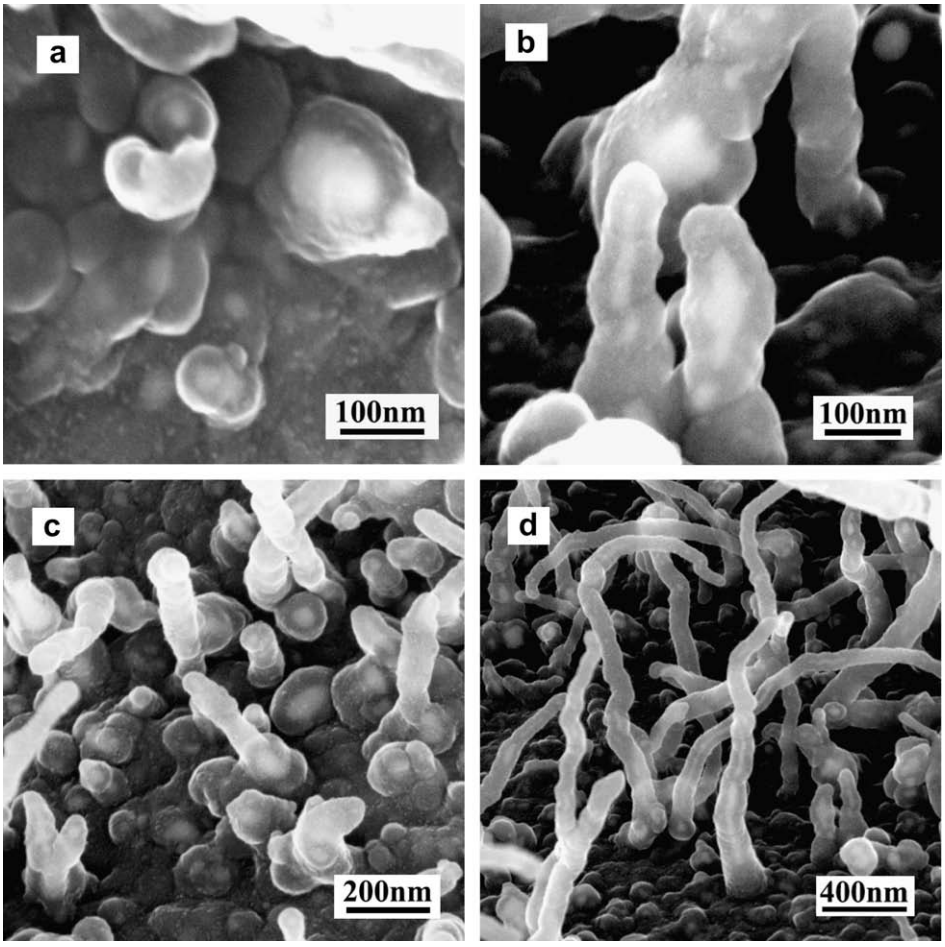

Fig. 11 – (a–d) SEM images of Fe-filled MWCNTs with gradually increasing length, showing that MWCNTs lengthen simultaneously with the filling of iron in their internal cavities.

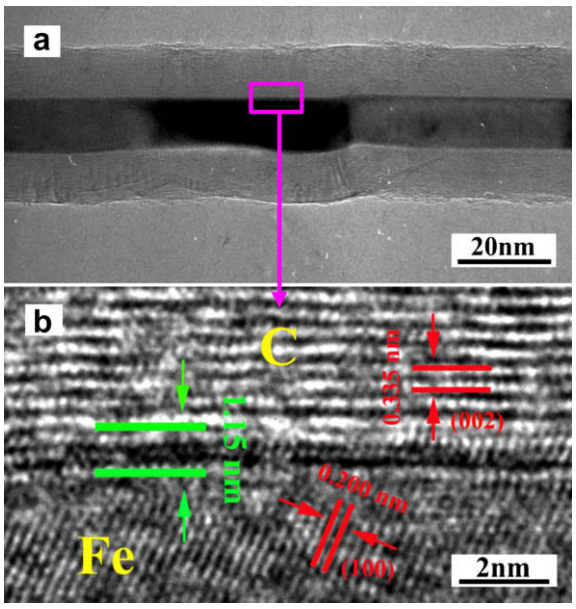

Fig. 12 – (a) TEM image of a Fe-filled MWCNT. (b) Enlarged TEM image of the framed portion in (a), showing the iron-nanotube interface.

tions can help iron to overcome the surface tension and enter the internal cavities of nanotubes.

The contact angle of most metals such as Pb on nanotube walls is normally >90°; however, closed nanotubes can be filled by molten lead in a reactive environment, because the fringe of Pb nanowires reacts with oxygen to form a compound with sufficiently low surface tension to be drawn in by capillarity [27]. In stark contrast, if nanotubes were opened and exposed to molten lead or other metals in an inert atmosphere, they would not draw in by capillarity [28]. We believe that the filling of Fe in MWCNTs is also for the similar phenomenon; i.e. the fringe of Fe nanowires reacts with carbon to form a thin-film compound with sufficiently low surface tension to fill in MWCNTs by capillarity. In the XRD diffraction patterns, a small fraction of iron carbide phases in the Fe-filled MWCNTs is always not completely eliminated, which is well in agreement with previously results [20]. Moreover, it is found that there always exists a highly distorted, amorphous-like and unidentified iron carbide phase within a layer approximately ~1 nm from the interface (Fig. 12). The highly ordered Fe single-crystal lattice fringes vanished in the area adjacent to the Fe-nanotube interface, which may belong to some superstructures, a variety of stable and metastable binary or ternary iron carbides, within nanoscale iron nanowires filled in the inner cavities of nanotubes. Such Fe-C superstructures were also observed by Golberg et al [20].

4. Conclusions

The pyrolysis of pure ferrocene has been systematically investigated at elevated temperature of ~1100 °C. The selective formation of various carbon nanostructures such as Fe-NPs adhering to SWCNTs, CNPs, Fe-NP decorated MWCNTs and Fe-filled MWCNTs by the pyrolysis of ferrocene is determined by the size of Fe particles as catalyst, which increases with T_{sub} of ferrocene. The magnetic characterization reveals that these nanostructures have an enhanced coercivity at room temperature, when compared to the bulk Fe. Moreover, by the pyrolysis of metallocenes such as ferrocene, nickelocene, cobaltocene, or their mixtures, this technology can be easily extended to prepare various magnetic nanostructures with tunable magnetic properties, which can find various applications in nanoelectronic devices, magnetic resonance imaging and magnetic data storage media.

Acknowledgements

The work was supported by Ministry of Science and Technology of China (No. 2006CB932701 and No. 2008DFA51400), National Science Foundation of China (No. 90606008 and No. 50702063), and Chinese Academy of Sciences (No. KJCX2-YW-M01).

REFERENCES

[1] Winkler A, Muhl T, Menzel S, Kozhuharova-Koseva R, Hampel S, Leonhardt A, et al. Magnetic force microscopy sensors using iron-filled carbon nanotubes. J Appl Phys 2006;99(10):104905-1–5.
[2] Monch I, Meye A, Leonhardt A, Kramer K, Kozhuharova R, Gemming T, et al. Ferromagnetic filled carbon nanotubes and nanoparticles: synthesis and lipid-mediated delivery into human tumor cells. J Magn Magn Mater 2005;290:276–8.
[3] Gudiksen MS, Lauhon LJ, Wang J, Smith DC, Lieber CM. Growth of nanowire superlattice structures for nanoscale photonics and electronics. Nature 2002;415(6872):617–20.
[4] Lauhon LJ, Gudiksen MS, Wang CL, Lieber CM. Epitaxial core-shell and core-multishell nanowire heterostructures. Nature 2002;420(6911):57–61.
[5] Subramoney S. Novel nanocarbons - Structure, properties and potential applications. Adv Mater 1998;10(15):1157–71.
[6] Grobert N, Hsu WK, Zhu YQ, Hare JP, Kroto HW, Walton DRM, et al. Enhanced magnetic coercivities in Fe nanowires. Appl Phys Lett 1999;75(21):3363–5.
[7] Muhl T, Elefant D, Graff A, Kozhuharova R, Leonhardt A, Monch I, et al. Magnetic properties of aligned Fe-filled carbon nanotubes. J Appl Phys 2003;93(10):7894–6.
[8] Leonhardt A, Ritschel M, Elefant D, Mattern N, Biedermann K, Hampel S, et al. Enhanced magnetism in Fe-filled carbon nanotubes produced by pyrolysis of ferrocene. J Appl Phys 2005;98(7):074315-1–5.
[9] Lu Y, Zhu ZP, Liu ZY. Carbon-encapsulated Fe nanoparticles from detonation-induced pyrolysis of ferrocene. Carbon 2005;43(2):369–74.
[10] Demoncy N, Stephan O, Brun N, Colliex C, Loiseau A, Pascard H. Filling carbon nanotubes with metals by the arc-discharge method: the key role of sulfur. Eur Phys J B 1998;4(2):147–57.
[11] Gao XP, Zhang Y, Chen X, Pan GL, Yan J, Wu F, et al. Carbon nanotubes filled with metallic nanowires. Carbon 2004;42(1):47–52.
[12] Rao CNR, Govindaraj A, Sen R, Satishkumar BC. Synthesis of multi-walled and single-walled nanotubes, aligned-nanotube bundles and nanorods by employing organometallic precursors. Mater Res Innov 1998;2(3):128–41.

[13] Rao CNR, Sen R, Satishkumar BC, Govindaraj A. Large aligned-nanotube bundles from ferrocene pyrolysis. Chem Commun 1998(15):1525–6.
[14] Schnitzler MC, Oliveira MM, Ugarte D, Zarbin AJG. One-step route to iron oxide-filled carbon nanotubes and bucky-onions based on the pyrolysis of organometallic precursors. Chem Phys Lett 2003;381(5–6):541–8.
[15] Pradhan BK, Kyotani T, Tomita A. Nickel nanowires of 4 nm diameter in the cavity of carbon nanotubes. Chem Commun 1999:1317–8.
[16] Liu SW, Wehmschulte RJ. A novel hybrid of carbon nanotubes/iron nanoparticles: iron-filled nodule-containing carbon nanotubes. Carbon 2005;43(7):1550–5.
[17] Liu QF, Ren WC, Li F, Cong HT, Cheng HM. Synthesis and high thermal stability of double-walled carbon nanotubes using nickel formate dihydrate as catalyst precursor. J Phys Chem C 2007;111(13):5006–13.
[18] Liu QF, Ren WC, Chen ZG, Liu BL, Yu B, Li F, et al. Direct synthesis of carbon nanotubes decorated with size-controllable Fe nanoparticles encapsulated by graphitic layers. Carbon 2008;46(11):1417–23.
[19] Muller C, Hampel S, Elefant D, Biedermann K, Leonhardt A, Ritschel M, et al. Iron filled carbon nanotubes grown on substrates with thin metal layers and their magnetic properties. Carbon 2006;44(9):1746–53.
[20] Golberg D, Mitome M, Muller C, Tang C, Leonhardt A, Bando Y. Atomic structures of iron-based single-crystalline nanowires crystallized inside multi-walled carbon nanotubes as revealed by analytical electron microscopy. Acta Mater 2006;54(9):2567–76.
[21] Morup S, Bodker F, Hendriksen PV, Linderoth S. Spin-Glass-Like Ordering of the Magnetic-Moments of Interacting Nanosized Maghemite Particles. Phys Rev B 1995;52(1):287–94.
[22] Bodker F, Morup S, Linderoth S. Surface effects in metallic iron nanoparticles. Phys Rev Lett 1994;72(2):282–5.
[23] Peng DL, Zhao X, Inoue S, Ando Y, Sumiyama K. Magnetic properties of Fe clusters adhering to single-wall carbon nanotubes. J Magn Magn Mater 2005;292:143–9.
[24] Hafner JH, Bronikowski MJ, Azamian BR, Nikolaev P, Rinzler AG, Colbert DT, et al. Catalytic growth of single-wall carbon nanotubes from metal particles. Chem Phys Lett 1998;296(1–2):195–202.
[25] Wei DC, Cao LC, Fu L, Li XL, Wang Y, Yu G, et al. A new technique for controllably producing branched or encapsulating nanostructures in a vapor-liquid–solid process. Adv Mater 2007;19(3):386–90.
[26] Dujardin E, Ebbesen TW, Hiura H, Tanigaki K. Capillarity and wetting of carbon nanotubes. Science 1994;265(5180):1850–2.
[27] Ajayan PM, Iijima S. Capillarity-induced filling of carbon nanotubes. Nature 1993;361(6410):333–4.
[28] Ajayan PM, Ebbesen TW, Ichihashi T, Iijima S, Tanigaki K, Hiura H. Opening carbon nanotubes with oxygen and implications for filling. Nature 1993;362(6420):522–55.